Electronic Supplementary Information (ESI)

Solvothermal synthesis and device fabrication of a Eu^{3+}-based metal-organic framework as a turn-on and blue-shift fluorescence sensor toward Cr^{3+}, Al^{3+} and Ga^{3+}

Yu Li, Ding-Gui Cai, Zi-Hao Zhu, Hui Xu,* Teng-Fei Zheng, Jing-Lin Chen, Sui-Jun Liu* and He-Rui Wen

School of Chemistry and Chemical Engineering, Jiangxi Provincial Key Laboratory of Functional Molecular Materials Chemistry, Jiangxi University of Science and Technology, Ganzhou 341000, Jiangxi Province, P.R. China.

*Corresponding authors. E-mail: sjliu@jxust.edu.cn (S.-J. Liu), xuhuijlu@163.com (H. Xu). Tel: +86-797-8312204.

CONTENTS

Section 1. Experimental Section

1. Materials and Instrumentations.

All starting materials including 5,5'-(benzo[c][1,2,5]thiadiazole-4,7-diyl) diisophthalic acid (H_4BTDI) were reagent grade and used by the purchase without further purification. The powder X-ray diffraction (PXRD) patterns were recorded on a Rigaku Miniflex 600 instrument. Elemental analysis (C, H, N and S) was performed on a vario EL cube elemental analyzer. The IR spectra were measured in the range of 4000-400 cm^{-1} with KBr pellets on a Bruker Alpha FT-IR spectrometer. Thermogravimetric analysis (TGA) was carried out on a NETZSCH STA2500 (TG/DTA) thermal analyzer under a N_2 flow at a heating rate of 10 °C min^{-1}. Fluorescence spectra were obtained using a F4600 (Hitachi) FL spectrophotometer. The ultraviolet visible (UV-vis) absorption spectra were collected on a UV-vis 2550 spectrophotometer. X-Ray photoelectron spectra (XPS) were recorded with an Axis Ultra DLD spectrometer. The amount of Cr^{3+}, Al^{3+} and Ga^{3+} ions in **JXUST-25** after sensing was measured on a HORIBA ULTIMA2 single channel instrument by inductive coupled plasma (ICP) emission spectroscopy analyses.

2. Crystallographic studies for JXUST-25.

Single-crystal X-ray diffraction data were obtained on a Bruker D8 QUEST diffractometer with Mo-Kα radiation (λ = 0.71073 Å) using ω scan mode. The SAINT program was used for integration of the diffraction profiles.[S1] The structure was solved with direct methods and refined by using full-matrix least squares on F^2 with SHELXL-2017/1.[S2] All non-H atoms were confirmed by successive difference Fourier syntheses and treated isotropically. Moreover, all hydrogen atoms were calculated in idealized positions on a geometric basis and refined with restrictions. The disorder atoms could be visible in ORTEP drawing of **JXUST-25** (Fig. S1b). Because of the limited crystal quality, the DMF molecule of **JXUST-25** has been masked. The summary of the crystal data and structural refinements of **JXUST-25** is provided in Table S1 (ESI) and Table 1. Selected bond lengths and bond angles of **JXUST-25** are listed in Table S2 (ESI).

Section 2. Supplementary Tables and Structural Figures

Table S1. Selected bond lengths (Å) and angles (°) for **JXUST-25**[a].

Eu1—O1^{i}	2.3189(15)	Eu1—O5^{iii}	2.3693(15)
Eu1—O2^{ii}	2.3796(15)	Eu1—O6^{iv}	2.3772(16)
Eu1—O4	2.4218(16)	Eu1—O7^{v}	2.4623(15)
Eu1—O3	2.5031(16)	Eu1—O8^{v}	2.5417(16)
O2^{ii}—Eu1—O1^{i}	125.20(6)	O6^{iv}—Eu1—O5^{iii}	128.11(5)
O3—Eu1—O1^{i}	83.26(5)	O7^{v}—Eu1—O1^{i}	96.31(5)
O3—Eu1—O2^{ii}	139.29(6)	O7^{v}—Eu1—O2^{ii}	125.57(6)
O4—Eu1—O1^{i}	134.74(6)	O7^{v}—Eu1—O3	70.20(6)
O4—Eu1—O2^{ii}	90.41(5)	O7^{v}—Eu1—O4	79.94(6)
O4—Eu1—O3	52.78(5)	O7^{v}—Eu1—O5^{iii}	149.33(6)
O5^{iii}—Eu1—O1^{i}	81.14(6)	O7^{v}—Eu1—O6^{iv}	79.37(5)
O5^{iii}—Eu1—O2^{ii}	77.86(6)	O8^{v}—Eu1—O1^{i}	139.17(5)
O5^{iii}—Eu1—O3	79.16(5)	O8^{v}—Eu1—O2^{ii}	73.95(5)
O5^{iii}—Eu1—O4	80.51(6)	O8^{v}—Eu1—O3	104.44(5)
O6^{iv}—Eu1—O1^{i}	74.47(6)	O8^{v}—Eu1—O4	71.35(6)
O6^{iv}—Eu1—O2^{ii}	80.08(6)	O8^{v}—Eu1—O5^{iii}	139.53(5)
O6^{iv}—Eu1—O3	139.80(5)	O8^{v}—Eu1—O6^{iv}	74.55(5)
O6^{iv}—Eu1—O4	145.90(6)	O8^{v}—Eu1—O7^{v}	52.11(5)

[a]Symmetry codes: (i) -*x*+1, -*y*, -*z*+2; (ii) *x*, *y*-1, *z*; (iii) -*x*+1, -*y*, -*z*+1; (iv) *x*, *y*-1, *z*+1; (v) -*x*, -*y*+1, -*z*+1.

Table S2. SHAPE analysis of Eu^{III} ions in **JXUST-25**.

ions	label	shape	symmetry	Distortion (τ)
	OP-8	Octagon	D_{8h}	32.730
	HPY-8	Heptagonal pyramid	C_{7v}	21.251
	HBPY-8	Hexagonal bipyramid	D_{6h}	15.558
	CU-8	Cube	O_h	9.048
	SAPR-8	Square antiprism	D_{4d}	2.876
	TDD-8	Triangular dodecahedron	D_{2d}	2.566
Eu1	JGBF-8	Johnson gyrobifastigium J26	D_{2d}	14.451
	JETBPY-8	Johnson elongated triangular bipyramid J14	D_{3h}	28.303
	JBTPR-8	Biaugmented trigonal prism J50	C_{2v}	2.554
	BTPR-8	**Biaugmented trigonal prism**	$\boldsymbol{C_{2v}}$	**1.633**
	JSD-8	Snub diphenoid J84	D_{2d}	5.178
	TT-8	Triakis tetrahedron	T_d	9.841
	ETBPY-8	Elongated trigonal bipyramid	D_{3h}	22.377

Table S3. The comparison of the detection limit between **JXUST-25** and some selected MOF sensors toward Cr^{3+}, Al^{3+} and Ga^{3+}.

Complex	Detection limit of Cr^{3+}	Detection limit of Al^{3+}	Detection limit of Ga^{3+}	Medium	luminescence effect	Ref.
$\{[(CH_3)_2NH_2][Eu(BTDI)]\cdot H_2O\cdot DMF\}_n$ (**JXUST-25**)	0.073 ppm (1.41 μM)	0.006 ppm (0.21μM)	0.030 ppm (0.44 μM)	DMF	Turn-on and blue-shift	**This work**
Tb-TCPP	9.94 nM (0.010 μM)	7.79 nM (0.008 μM)	-	DMF	Turn-on	S3
$\{[Zn(BIBT)(oba)]\cdot DMA\}_n$ (**JXUST-3**)	0.049 μM	0.055 μM	-	EtOH	Turn-off	S4
$\{[Co_3(BIBT)_3(BTC)_2(H_2O)_2]\cdot solvents\}_n$ (**JXUST-2**)	0.10 μM	0.10μM		DMAc	Turn-on	S5
$[Zn_2(5\text{-}NH_2\text{-}1,3\text{-}bdc)_2(NI\text{-}bpy\text{-}44)]\cdot DMF$	7.87 μM	5.59 μM	-	H_2O	Turn-off	S6
$\{[Tb_2(ADIP)(H_2ADIP)(HCOOH)(H_2O)_2]\cdot 2DMF\cdot 2H_2O\}_n$	-	0.069 μM	0.079 μM	EtOH	Turn-on and blue-shift	S7
$\{[Cd(BBZB)(2,6\text{-}NDC)]\cdot CH_3OH\}_n$ (**JXUST-6**)	-	0.081 ppm	0.047 ppm	DMF	Turn-on and red-shift	S8
$\{[Zn_2(BBIP)_2(NDC)_2]\cdot H_2O\}_n$ (**JXUST-5**)	-	0.17 ppm	0.69 ppm	EtOH	Turn-on and red-shift	S9
$\{[(CH_3)_2NH_2][Eu(BTDB)_2]\cdot 2H_2O\}_n$ (**JXUST-11**)	-	2.9 ppm	10.2 ppm	DMF	Turn-on	S10

References

S1 *SAINT*, *Version 6.02a*, Bruker AXS Inc, Madison, WI, 2002.

S2 G. M. Sheldrick, *Acta Crystallogr. Sect. A: Found. Adv.,* 2015, **A71**, 3-8.

S3 C. Fu, X. Sun, G. Zhang, P. Shi and P. Cui, *Inorg. Chem.*, 2021, **60**, 1116-1123.

S4 S. L. Yao, Y. C. Xiong, X. M. Tian, S. J. Liu, H. Xu, T. F. Zheng, J. L. Chen and H. R. Wen, *CrystEngComm*, 2021, **23**, 1898-1905.

S5 X. M. Tian, S. L. Yao, C. Q. Qiu, T. F. Zheng, Y. Q. Chen, H. Huang, J. L. Chen, S. J. Liu and H. R. Wen, *Inorg. Chem.*, 2020, **59**, 2803-2810.

S6 J. R. Zhang, J. J. Lee, C. H. Su, M. J.; Tsai, C. Y. Li and J. Y. Wu, *Dalton Trans.*, 2020, **49**, 14201-14215.

S7 T. L. Ren, X. N. Zhang, J. J. Hu, H. R. Wen, S. J. Liu and Y. Peng, *Dalton Trans.*, 2022, **51**, 14858-14864.

S8 B. L. Chai, S. L. Yao, X. Xie, H. Xu, T. F. Zheng, J. Y. Li, J. L. Chen, S. J. Liu and H. R. Wen, *Cryst. Growth Des.*, 2022, **22**, 277-284.

S9 L. H. Wu, S. L. Yao, H. Xu, T. F. Zheng, S. J. Liu, J. L. Chen, N. Li and H. R. Wen, *Chin. Chem. Lett.*, 2022, **33**, 541-546.

S10 J. Li, Y. L. Zhu, H. Xu, T. F. Zheng, S. J. Liu, Y. Q. Wu, J. L. Chen, Y. Q. Chen and H. R. Wen, *Inorg. Chem.*, 2022, **61**, 3607-3615.

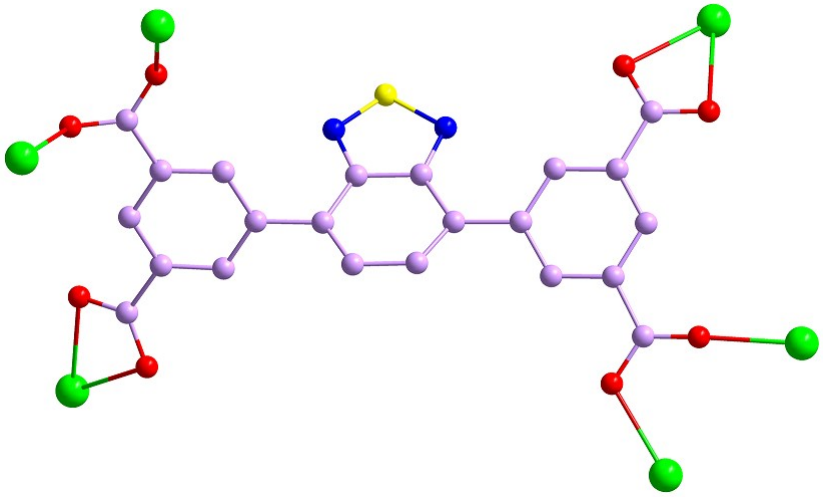

(a)

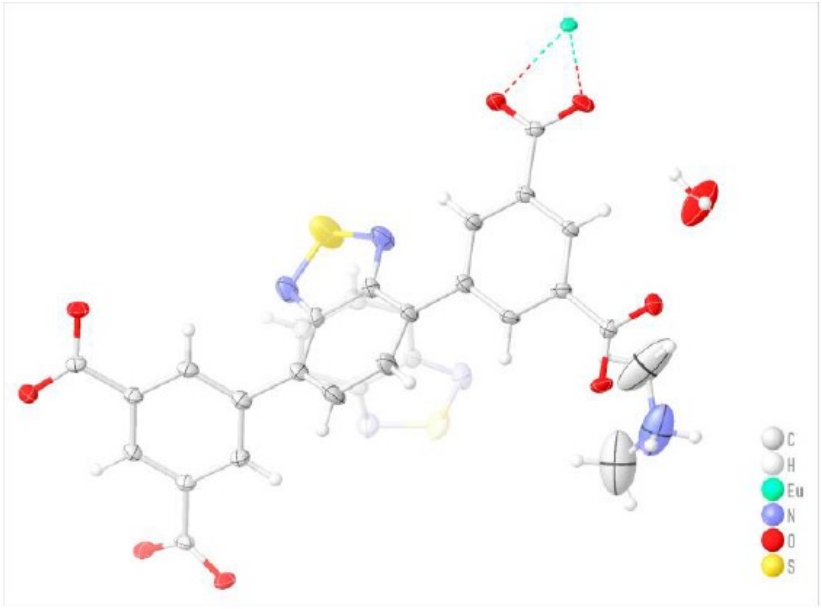

(b)

Fig. S1 (a) The coordination mode of $BTDI^{4-}$ ligand in **JXUST-25**. (b) The probability ORTEP drawing of the asymmetric unit of **JXUST-25**.

Section 3. Supplementary Characterizations

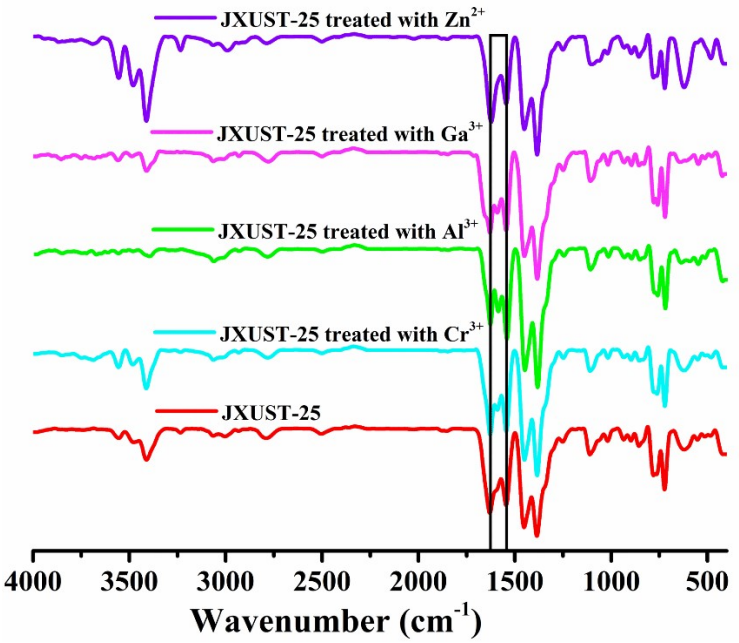

Fig. S2 The IR spectra of **JXUST-25** before and after treated with Cr^{3+}, Al^{3+}, Ga^{3+} and Zn^{2+} at room temperature.

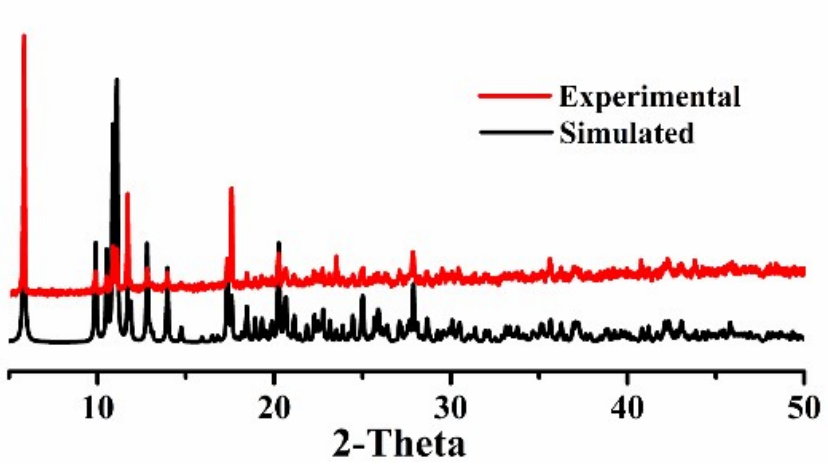

(a)

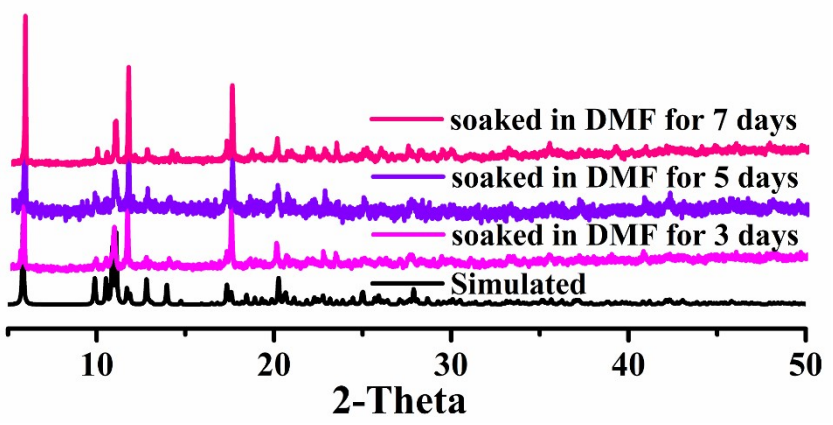
soaked in DMF for 7 days
soaked in DMF for 5 days
soaked in DMF for 3 days
Simulated
10
20
30
40
50
2-Theta

(b)

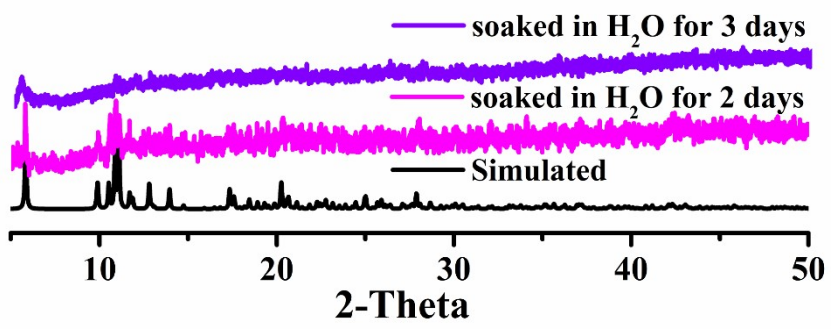
soaked in H2O for 3 days
soaked in H2O for 2 days
Simulated
10
20
30
40
50
2-Theta

(c)

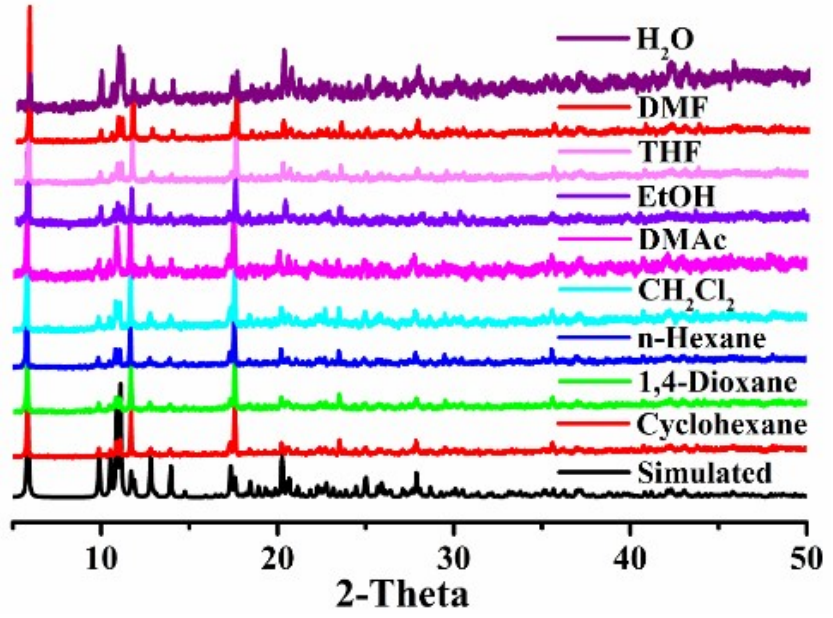
H2O
DMF
THF
EtOH
DMAc
CH2Cl2
n-Hexane
1,4-Dioxane
Cyclohexane
Simulated
10
20
30
40
50
2-Theta

(d)

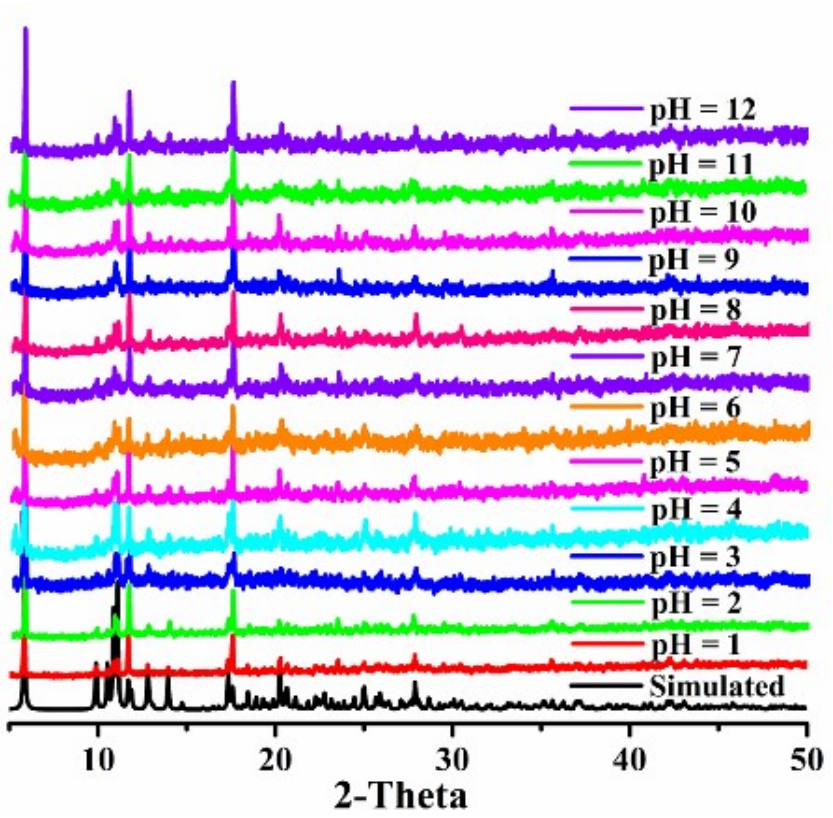

(e)

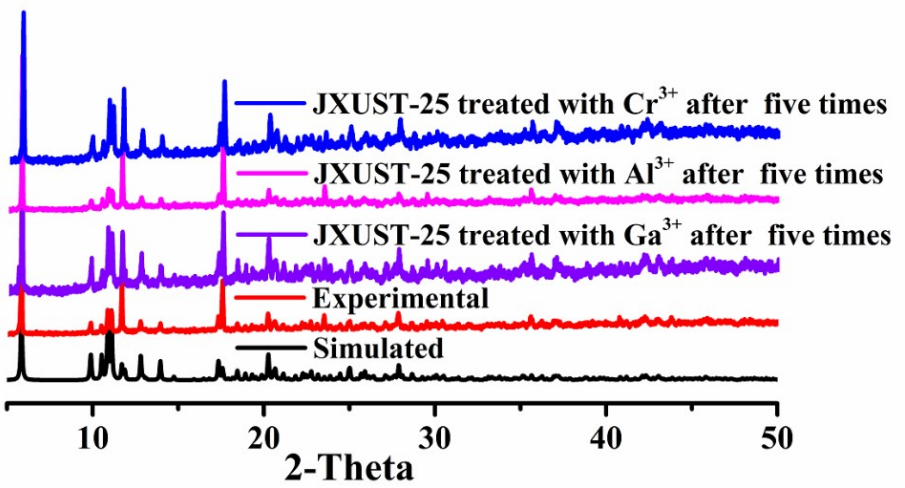

(f)

Fig. S3 The simulated and experimental PXRD patterns of (a) the as-synthesized sample of **JXUST-25**; (b) the samples of **JXUST-25** soaked in DMF for 3, 5 and 7 days; (c) the samples of **JXUST-25** soaked in DMF for 2 and 3 days; (d) the samples of **JXUST-25** immersed in common solvents for 24 h; (e) **JXUST-25** in aqueous solution with different pH values for 6 h; (f) **JXUST-25** after sensing Cr^{3+}, Al^{3+} and Ga^{3+} for 5 cycles.

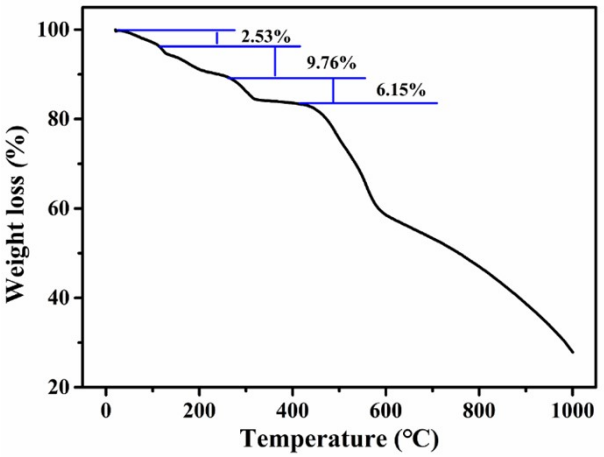

Fig. S4 The TGA curve for **JXUST-25** under N_2 atmosphere.

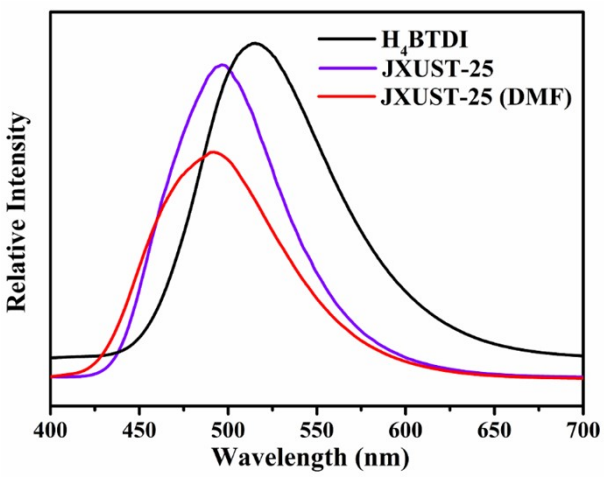

(a)

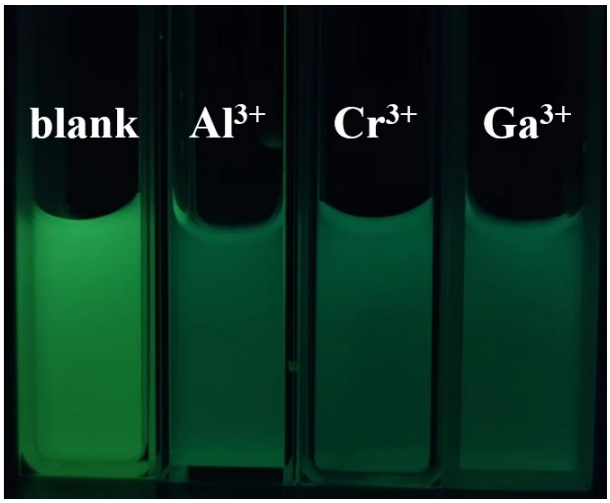

(b)

Fig. S5 (a) The emission spectra of H_4BTDI and **JXUST-25** in the solid state and in DMF solution (λ_{ex} = 368 nm); (b) the naked-eye photographs of **JXUST-25** dispersed in the aqueous solution containing Al^{3+}, Cr^{3+} and Ga^{3+} under UV-lamp with the wavelength of 365 nm.

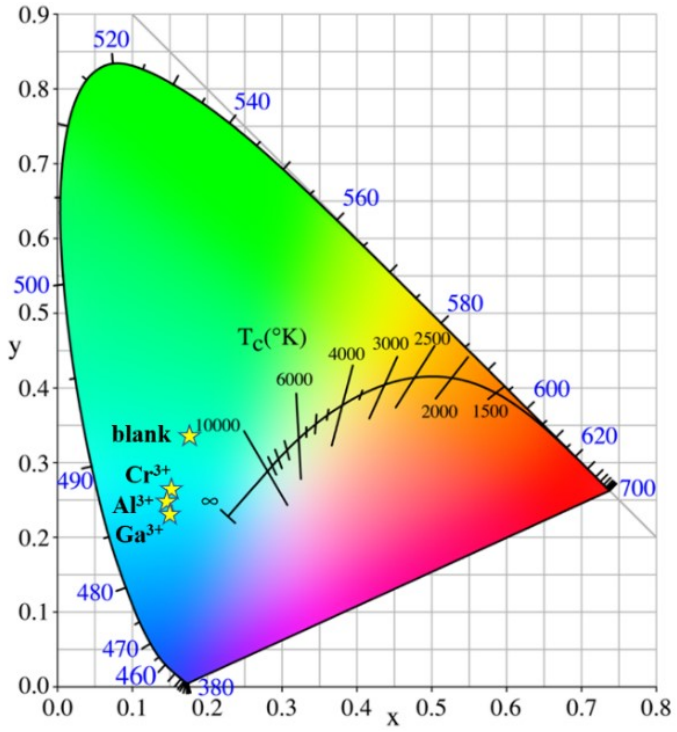

Fig. S6 CIE chromaticity diagram showing the color coordinates of **JXUST-25** upon the addition of Cr^{3+}, Al^{3+} and Ga^{3+}.

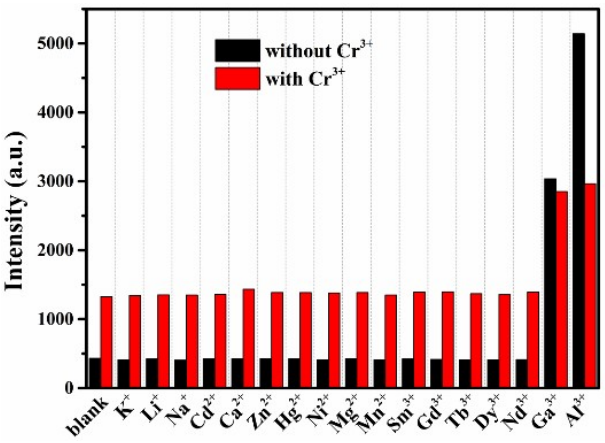

(a)

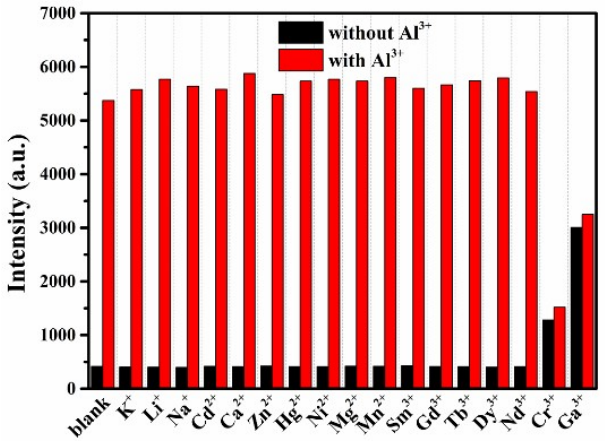

(b)

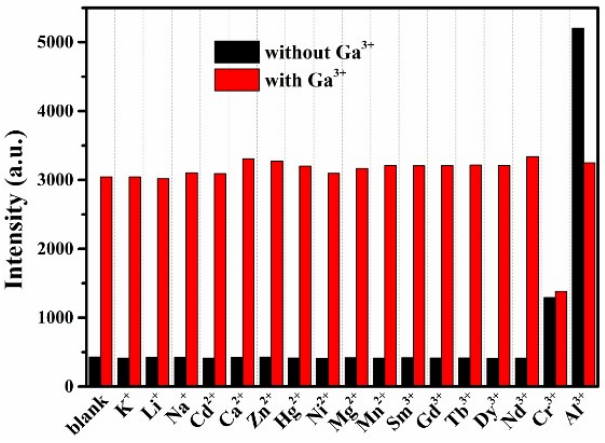

(c)

Fig. S7 Competitive experiments of **JXUST-25** in sensing (a) Cr^{3+}, (b) Al^{3+} and (c) Ga^{3+} with the interference of other metal ions (0.2 M) in DMF solution.

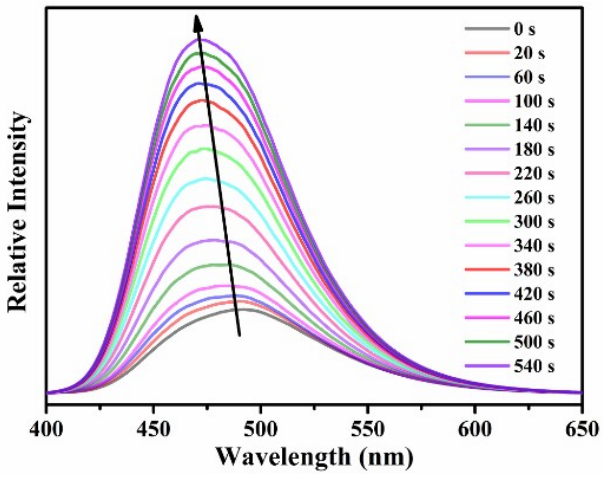

(a)

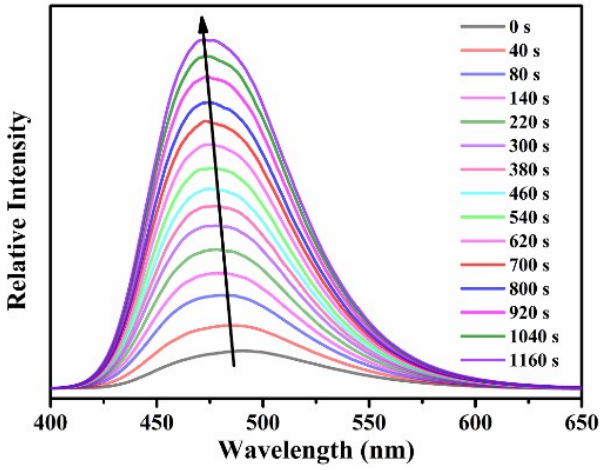

(b)

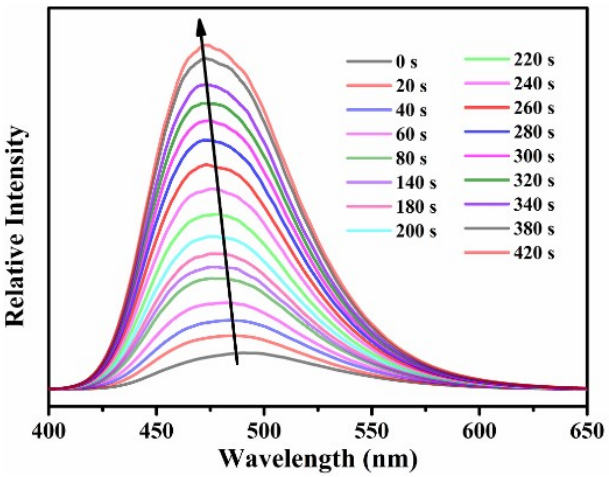

(c)

Fig. S8 Time-dependent emission spectra of **JXUST-25** in DMF suspension after adding (a) Cr^{3+} (5×10^{-4} mol/L), (b) Al^{3+} (5×10^{-4} mol/L) and (c) Ga^{3+} (5×10^{-4} mol/L) at room temperature.

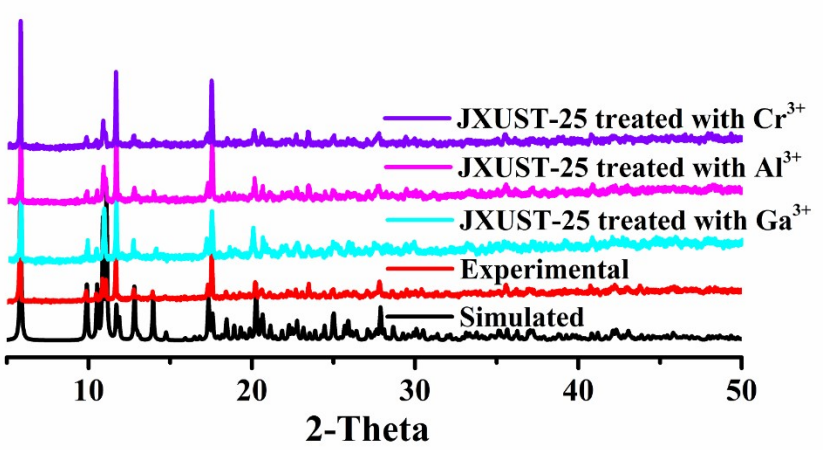

Fig. S9 The PXRD patterns of **JXUST-25** in DMF solution after adding Cr^{3+}, Al^{3+} and Ga^{3+} for 24 h.

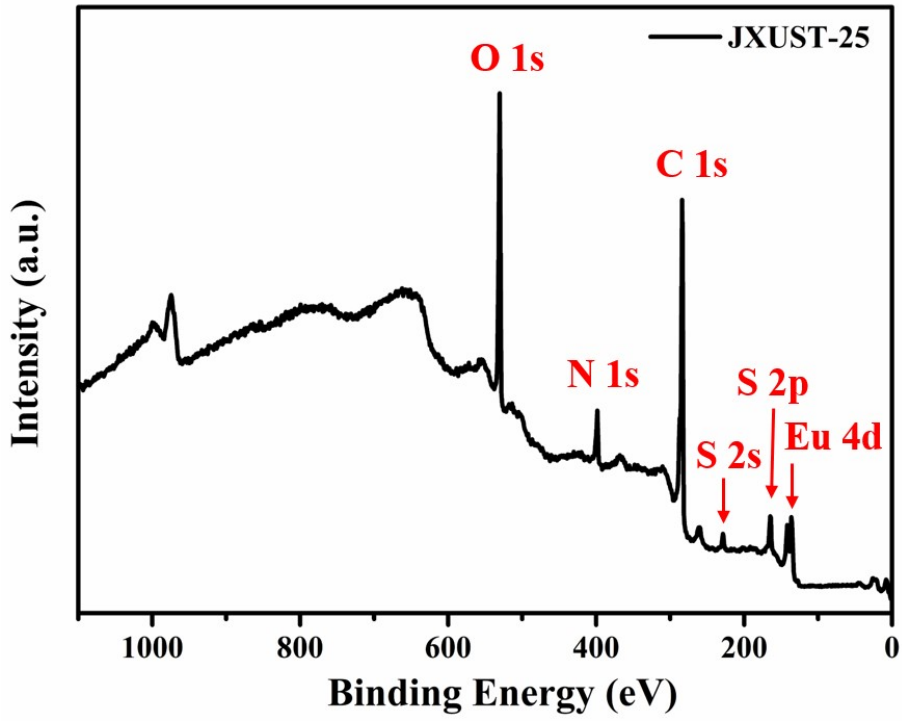

(a)

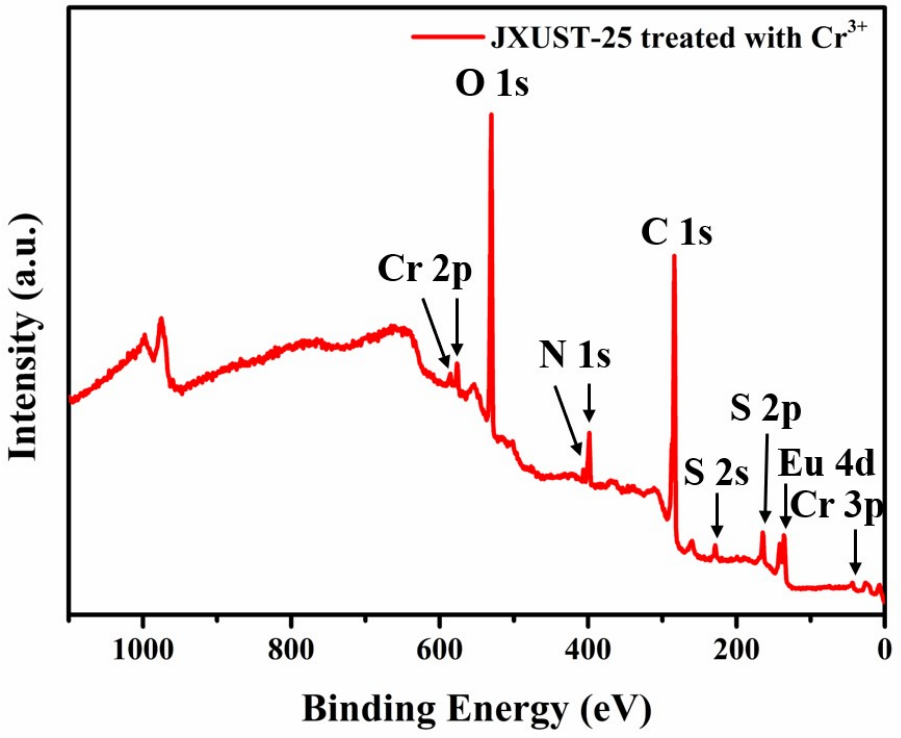
JXUST-25 treated with Cr3+
O 1s
C 1s
Cr 2p
N 1s
S 2p
S 2s
Eu 4d
Cr 3p
Intensity (a.u.)
1000
800
600
400
200
0
Binding Energy (eV)

(b)

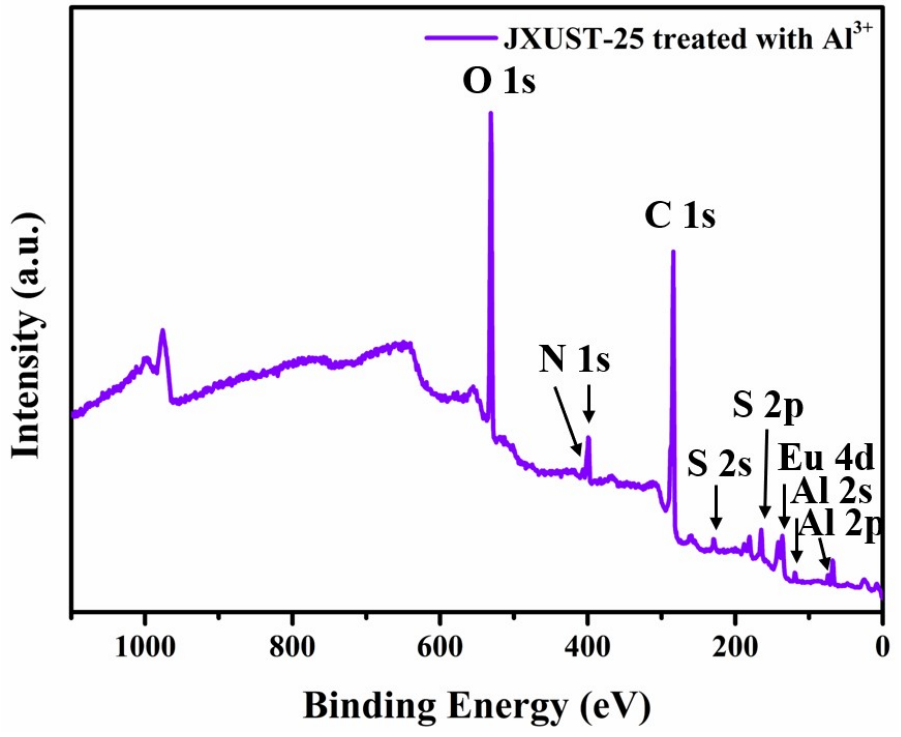
JXUST-25 treated with Al3+
O 1s
C 1s
N 1s
S 2p
S 2s
Eu 4d
Al 2s
Al 2p
Intensity (a.u.)
1000
800
600
400
200
0
Binding Energy (eV)

(c)

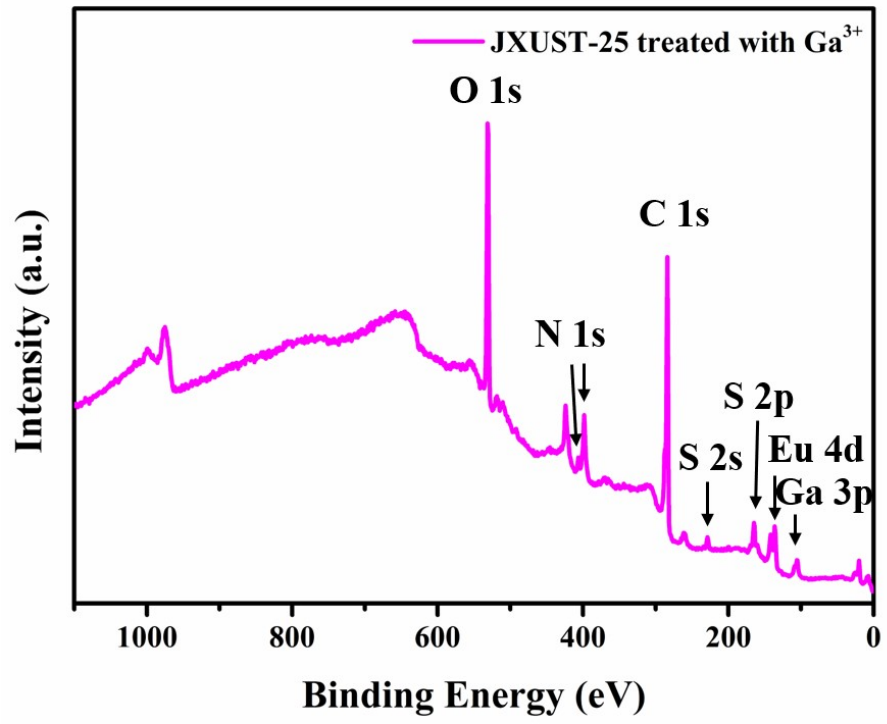

(d)

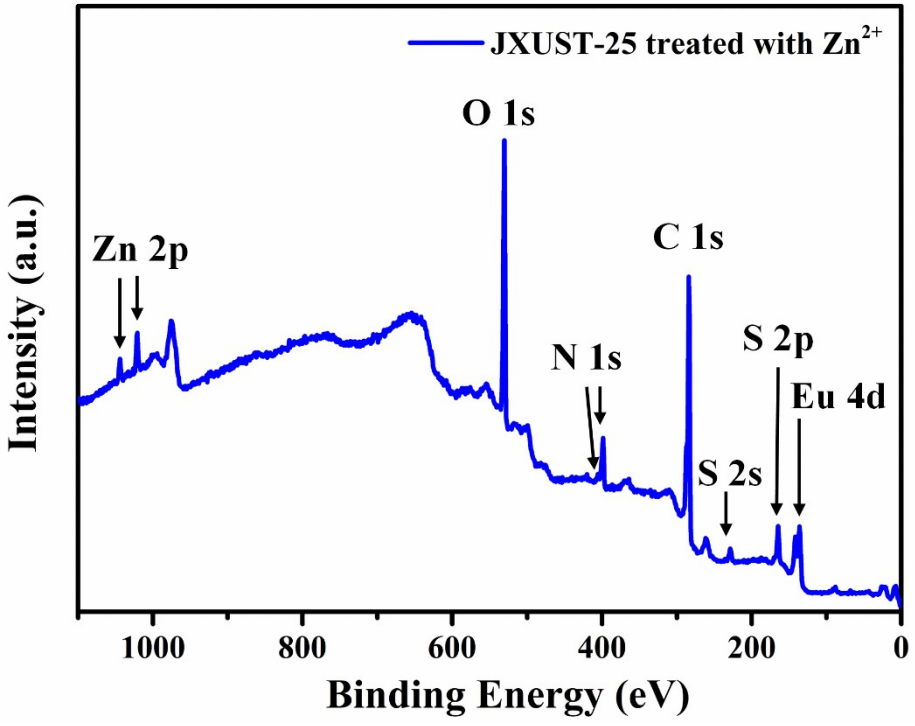

(e)

Fig. S10 XPS of (a) **JXUST-25**, (b) **JXUST-25** treated with Cr^{3+}, (c) **JXUST-25** treated with Al^{3+}, (d) **JXUST-25** treated with Ga^{3+}, and (e) **JXUST-25** treated with Zn^{2+}. The samples of **JXUST-25** were soaked in 1 mM Cr^{3+}, Al^{3+}, Ga^{3+} and Zn^{2+} solutions for 24 h.

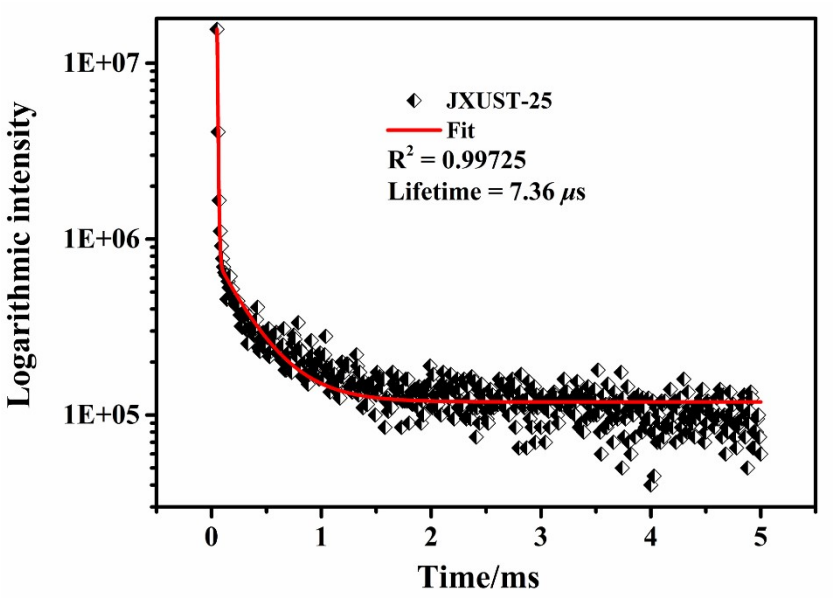
1E+07
1E+06
1E+05
Logarithmic intensity
JXUST-25
Fit
R2 = 0.99725
Lifetime = 7.36 μs
0
1
2
3
4
5
Time/ms

(a)

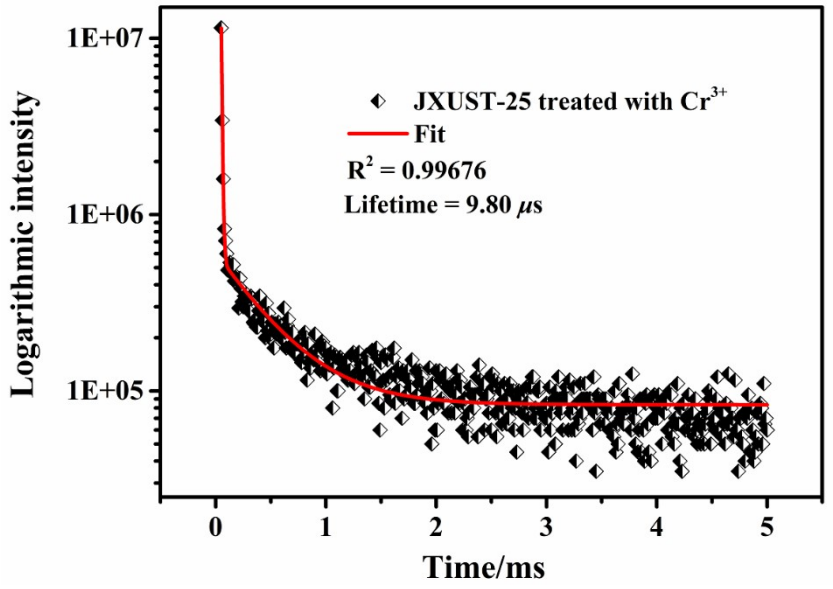
1E+07
1E+06
1E+05
Logarithmic intensity
JXUST-25 treated with Cr3+
Fit
R2 = 0.99676
Lifetime = 9.80 μs
0
1
2
3
4
5
Time/ms

(b)

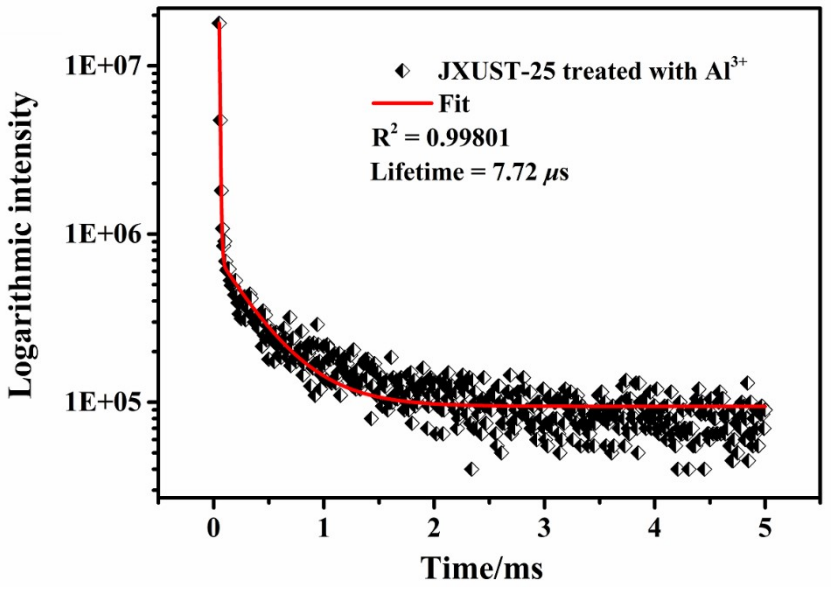

(c)

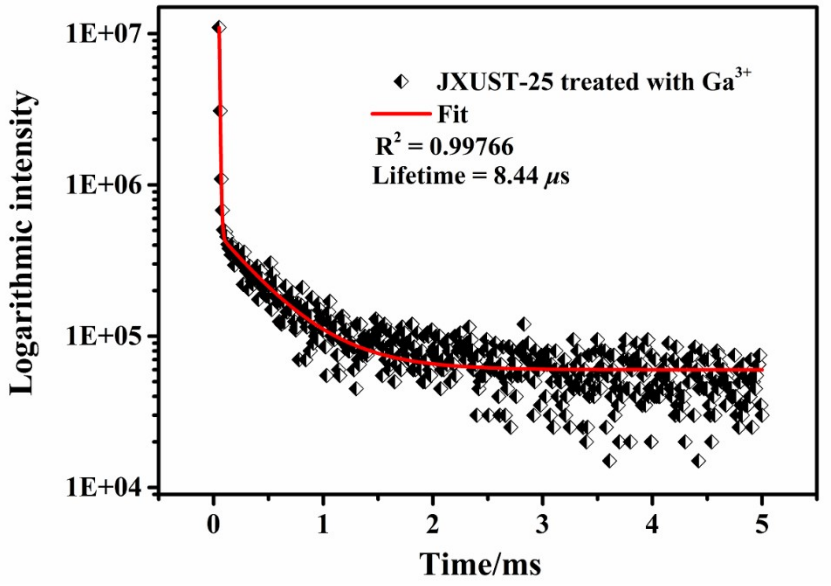

(d)

Fig. S11 The luminescence decay curves of (a) **JXUST-25**, (b) **JXUST-25** treated with Cr^{3+}, (c) **JXUST-25** treated with Al^{3+} and (d) **JXUST-25** treated with Ga^{3+} at room temperature.

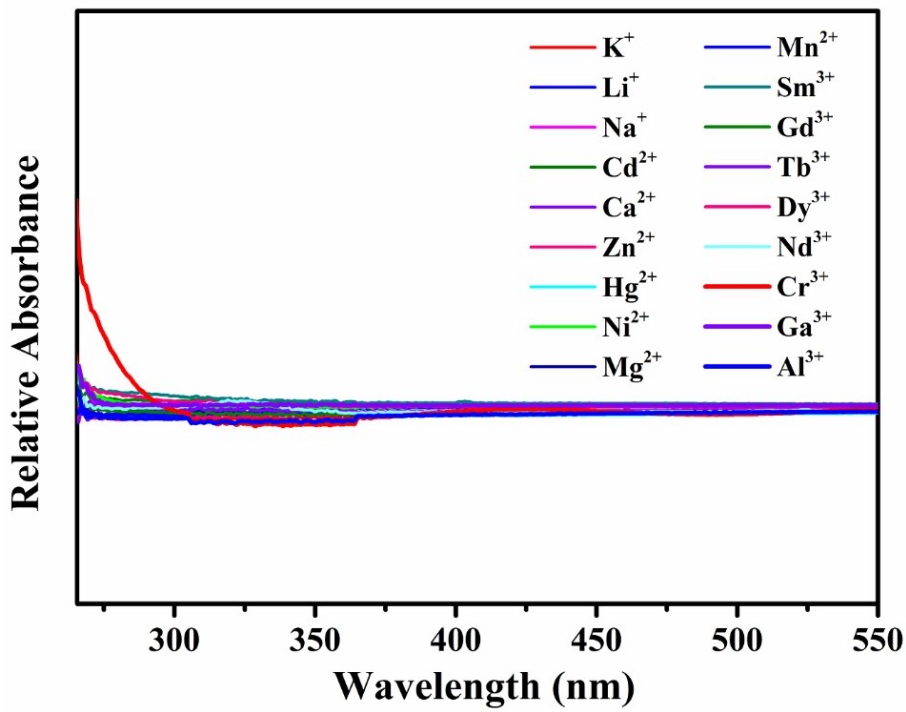

Fig. S12 UV-vis absorption spectra of different metal ions in DMF solutions.

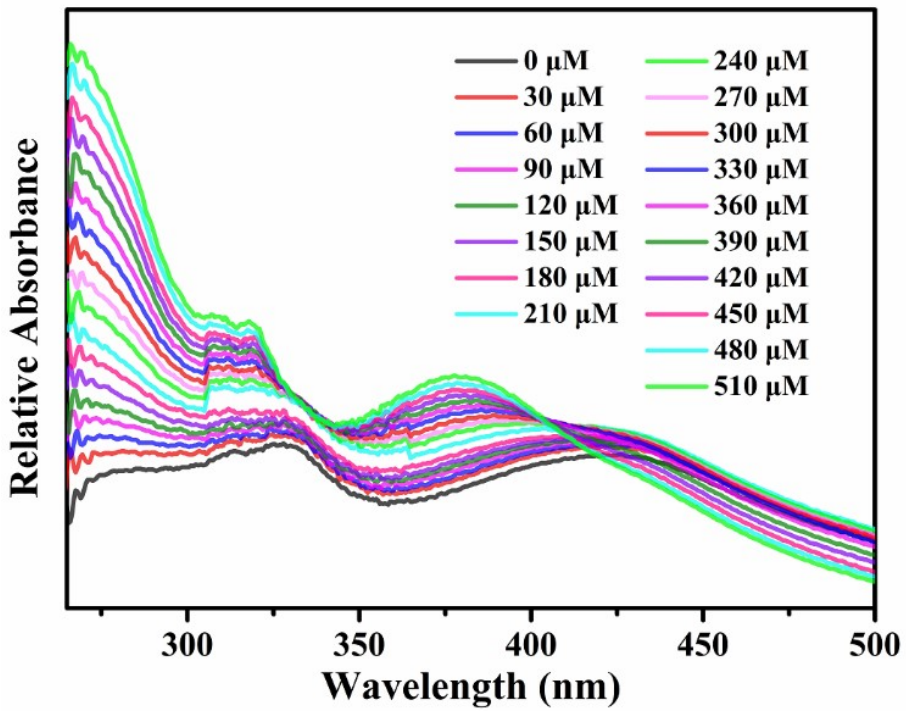

(a)

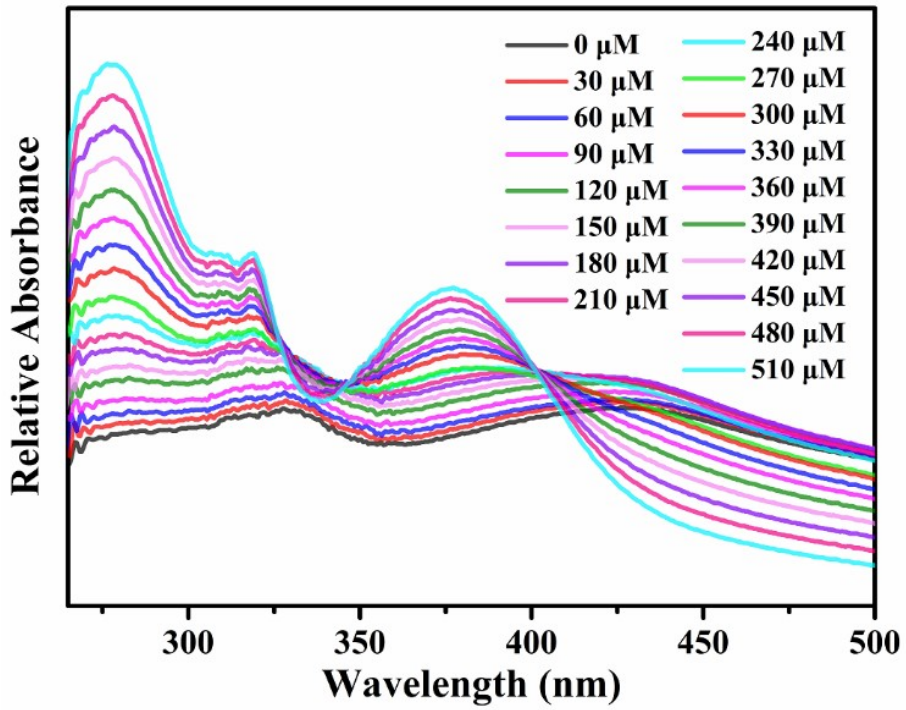

(b)

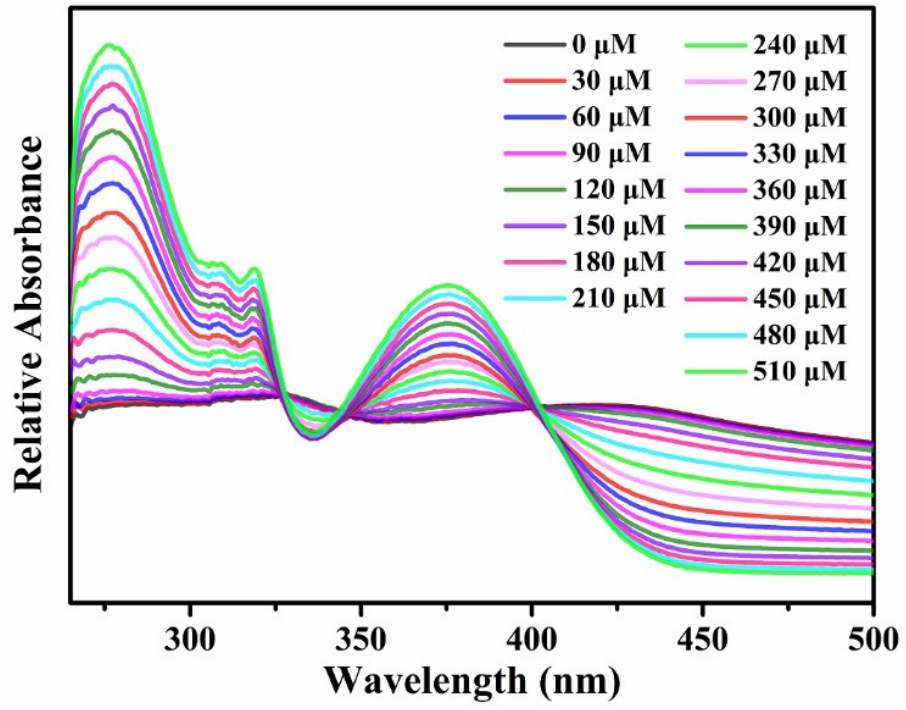

(c)

Fig. S13 The UV-vis absorption spectra of **JXUST-25** dispersed in DMF solution after adding different concentration of (a) Cr^{3+}, (b) Al^{3+} and (c) Ga^{3+}.